ACTA ODONTOLOGICA SCANDINAVICA
2018, VOL. 76, NO. 4, 247–252
https://doi.org/10.1080/00016357.2017.1412498

Taylor & Francis
Taylor & Francis Group

ORIGINAL ARTICLE

Cone beam computed tomography imaging of superior semicircular canal morphology: a retrospective comparison of cleft lip/palate patients and normal controls

Oğuzhan Altun[a], Suayip Burak Duman[a], Ibrahim Sevki Bayrakdar[b], Yasin Yasa[c], Sacide Duman[d] and Sevcihan Günen Yılmaz[e]

[a]Department of Oral and Maxillofacial Radiology, Faculty of Dentistry, Inönü University, Malatya, Turkey; [b]Department of Oral and Maxillofacial Radiology, Faculty of Dentistry, Eskişehir Osmangazi University, Eskişehir, Turkey; [c]Department of Oral and Maxillofacial Radiology, Faculty of Dentistry, Ordu University, Ordu, Turkey; [d]Department of Pedodontics, Faculty of Dentistry, Inönü University, Malatya, Turkey; [e]Department of Oral and Maxillofacial Radiology, Faculty of Dentistry, Akdeniz University, Antalya, Turkey

ABSTRACT

Objective: This study evaluated the prevalence and morphological characteristics of the superior semicircular canal (SSCC) in cleft lip and palate (CL/P) patients using cone beam computed tomography (CBCT).

Materials and methods: CBCT images of 53 CL/P patients (28 males and 25 females) and a control group of 76 patients (42 males and 34 females) were evaluated. Retrospectively, 258 temporal bone images from 129 patients were evaluated in terms of SSCC morphology and divided into a normal pattern (0.6–1.7 mm in thickness), a papyraceous pattern (<0.5 mm), a thick pattern (>1.8 mm), a pneumatized pattern and dehiscent. The chi-squared test was used to compare differences among semicircular canal dehiscence (SSCD) patterns in the CL/P and control groups; $p \leq .05$ was taken to reflect statistical significance.

Results: The characteristics of the SSCC were evaluated on CBCT images in patients with CL/P and controls. In total, 158 (61%) cases were normal (0.6–1.7 mm in thickness), 31 (12%) papyraceous (<0.5 mm), 8 (3%) thick, and 34 (13%) pneumatized. SSCD was observed in 27 (11%) cases. Statistically significant differences between the CL/P and control groups were evident in terms of SSCC morphology ($p < .001$).

Conclusions: SSCD should be considered if a CL/P patient exhibits a vestibular system deficiency. Oral and maxillofacial radiologists should pay attention to SSCD when interpreting CBCT images. Future studies should use high-level spatial resolution CBCT to focus on cleft site and SSCC morphology in larger patient populations.

ARTICLE HISTORY
Received 18 July 2017
Revised 14 October 2017
Accepted 28 November 2017

KEYWORDS
Semicircular canal morphology; cone beam computed tomography; cleft lip and palate

Introduction

Cleft lip and palate (CL/P) is a common birth defect (~9.1 cases per 10,000 births) and varies by ethnic group, geographical location and socioeconomic conditions [1]. A cleft palate is attributable to complete or incomplete assembly of the medial nasal prominence(s) on one or both sides [2]. A CL/P compromises hearing, speech and facial configuration. For several reasons, it is essential to explore the relationship between CL/P and other malformations. In addition, the association of CL/P with other congenital anomalies would increase our understanding of the embryogenic situation underlying the malformation [3]. Children with CL/P experience feeding difficulties, dental anomalies (e.g. tooth agenesis or supernumary teeth) and an increased risk of infection; they may also eventually develop speech and socio-psychological problems because they are stigmatized. A CL/P occurs more often in newborn males than females. Although facial regions near the cleft may experience delayed growth, surgical intervention allows individuals born with a CL/P to exhibit craniofacial, catch-up skeletal growth [4,5]. As a CL/P can affect maxillofacial bone structure, we explored whether semicircular canal dehiscence (SSCD) is more common in CL/P patients than normal controls.

The vestibular system is composed of three semicircular canals (SSCs) and otoliths in the temporal bone. The SSCs run in the posterior, superior and horizontal planes of the bony labyrinth of the inner ear. Each SSC is at a 90° angle to the others. The superior semicircular canal (SSCC) is a component of the vestibular system, regulating rotation of the head around the anteroposterior axis [6,7]. SSCD reflects the absence of bone overlying the SSC and is rare in the absence of lateral canal involvement [6,8–10]. SSCD was first identified by Minör et al. [11] in 1998 as a specific clinical abnormality of the temporal bone [11]. SSCD can cause both vestibular and cochlear symptoms. Auditory symptoms include hyperacusis, tinnitus, aural fullness, and autophony. Vertigo or

CONTACT Ibrahim Sevki Bayrakdar ibrahimsevkibayrakdar@gmail.com Department of Oral and Maxillofacial Radiology, Faculty of Dentistry, Osmangazi University, Eskişehir 26480, Turkey

nystagmus evoked by load noise (the Tullio phenomenon), oscillopsia, changes in middle ear pressure, and disequilibrium caused by sound or changes in intracranial pressure are among the vestibular symptoms of such patients [10,12–15]. Also, SSCD may afford a pathway for the intracranial spread of infection [16].

Chausse was the first to image the SSC in 1943 [6]. Later, various projections, including the Schüller II projection (petrous bones in the orbits), Towne projection (semi-axial), and Stenvers projection (occipitozygomatic) were described. High-resolution computed tomography (CT) is the most common imaging method used to examine the SSCC [14,17–22]. A diagnosis of SSCD is based on the presence of vestibular or auditory symptoms. Key components of the diagnosis are confirmed via high-resolution CT [17]. Minör et al. [11] reported that CT identified SSCD with a sensitivity of 100% and a specificity of 99% [12]. However, it is generally agreed that routine CT does not yield a definitive diagnosis of SSCD because of limitations in resolution. Routine CT cannot detect a bony layer <0.1 mm in thickness. Currently, cone beam computed tomography (CBCT) is widely used to diagnostically image the head and neck region. Although CBCT is a relatively new radiological technique, it has become very useful. CBCT enables three-dimensional (3D) data acquisition, followed by image reconstruction, display and interpretation. CBCT scans are rapid and deliver only low doses of radiation, rendering the modality ideal for imaging children and claustrophobic adults [23]. As CBCT can be performed with the patient standing or sitting, the patient feels comfortable [24,25]. CBCT has been shown to be at least as good as CT when used to examine bone structures (e.g. the skull base, paranasal sinuses and temporal bone) and pathologies in the oral and maxillofacial region [26]. Although CBCT is commonly used by dentists, otolaryngologists also favor the technique because of the good imaging quality afforded [26]. CBCT is also preferred when evaluating cases of dysplasia, traumatic lesions, erosion of the thin osseous labyrinthine wall and dehiscence [27,28]. Bremke et al. [29] showed that, *in vitro*, CBCT was significantly better than high-resolution CT in identifying thin bony coverage of the SSC in temporal bone specimens.

The etiology of SSCD remains unclear; several views have been published. Nadgir et al. [30] argued that SSCD was not congenital, but later studies reported congenital abnormalities [31,32]. According to Carey et al. [33], the symptoms and signs of SSCD first develop in adulthood. The cited authors suggested that trauma or increased cerebrospinal fluid pulsation attributable to a rise in intracranial pressure might cause SSCD. Others have suggested that SSCD is caused by abnormalities in bone deposition during childhood and adolescence [7,20,33,34]. The aim of this study was to evaluate the frequency and morphological characteristics of the SSCC in CL/P patients using CBCT.

Materials and methods

The CBCT images of 53 individuals (28 males and 25 females) with CL/P (40 unilateral and 13 bilateral patients) were obtained at the Faculty of Dentistry, Inonü University, Malatya, Turkey. For comparison, we evaluated a control group of 76 randomly selected patients (42 males and 34 females) in the same age range as the CL/P group for whom CBCT was performed for any other reason, including tooth impaction, temporomandibular joint problems, and a bone pathology, etc. We retrospectively evaluated 258 temporal bone images from 129 patients in terms of the morphological characteristics of the SSCC. This study was performed according to the principles of the Helsinki Declaration; all study subjects signed informed consent forms.

CBCT imaging

CBCT images were acquired with the patients in the standard supine position (scanning time, 14–18 s, field of view 18×13 cm; exposure time 3.6 s, kVp = 110, mA = 1–11; voxel size 0.2 mm^3) using the same device (NewTom 5G, QR Verona, Verona, Italy). To ensure a consistent orientation of the sagittal images, the head was placed with the Frankfort horizontal plane perpendicular to the table and the entire head within the circular gantry housing the X-ray tube. All images were analyzed with the aid of Quantitative Radiology (QR) NNT version 2.21 imaging software.

CBCT image evaluation

CBCT images were first taken in the axial plane. Using these images, the Pöschl and Stenvers planes were reformatted. The Pöschl plane runs at approximately a 45° angle to both the coronal and sagittal planes and was specifically drawn parallel to the SSCC (Figure 1). In this plane, the SSCC appears as an intact ring. The Stenvers plane lies perpendicular to the Pöschl plane, and is also at approximately a 45° angle to both the coronal and sagittal planes, providing a clear image of the roof of the SSCC (Figure 2).

In each temporal bone, minimum thickness of the bone covering the roof of the SSC was measured the adjacent to the middle fossa. The minimum thickness of bone overlying the SSC has been defined as thinnest point of bone observed on CBCT slices achieved in the Pöschl plane as the SSC, between the outer surface of the SSC and the free surface of the middle cranial fossa. All SSCCs were evaluated in all three planes (the axial, Pöschl and Stenvers planes) and were categorized as described by Cisneros et al. [17] as follows:

- *Normal pattern* (Figure 3(A)): the SSCC was 0.6–1.7 mm in thickness;
- *Papyraceous pattern* (Figure 3(B)): the SSCC was characterized by a fine thin cover of bone <0.5 mm in thickness;
- *Thick pattern* (Figure 3(C)): the SSCC was >1.8 mm in thickness;
- *Pneumatized pattern* (Figure 3(D)): the roof of the canal featured multiple supralabyrinthine cells, presenting as a woven structure;
- *Dehiscent pattern* (Figure 3(E)): the SSCC was characterized by a break in the bony cover of the canal. The SSCC length was measured in the Pöschl plane.

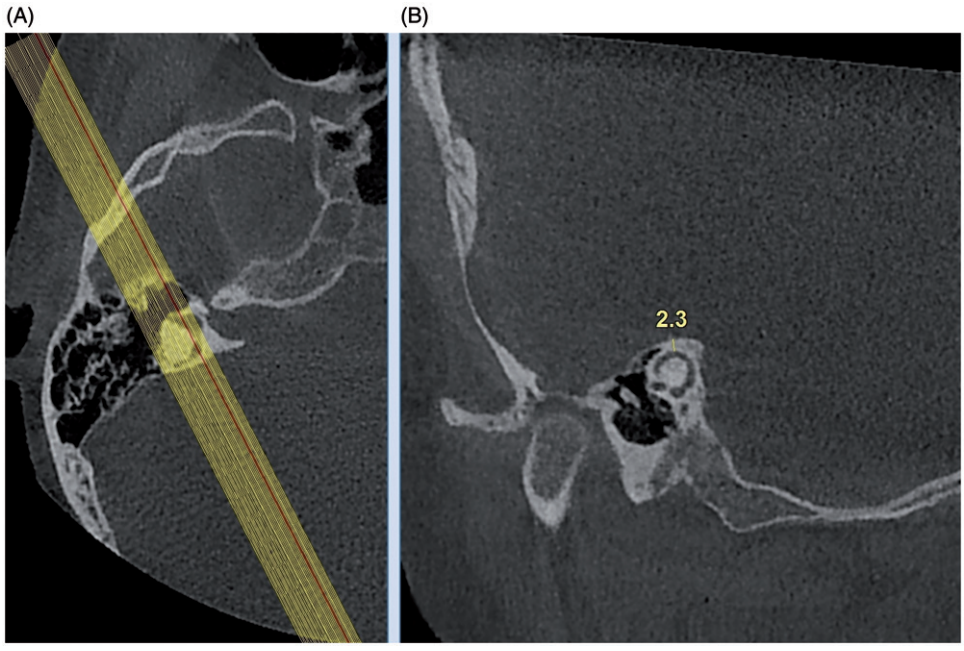

Figure 1. Cone beam computed tomography images. (A) Pöschl plane. Angle of reformation showed on axial CBCT image. (B) Normal features are seen as a whole ring on axial reformatted image.

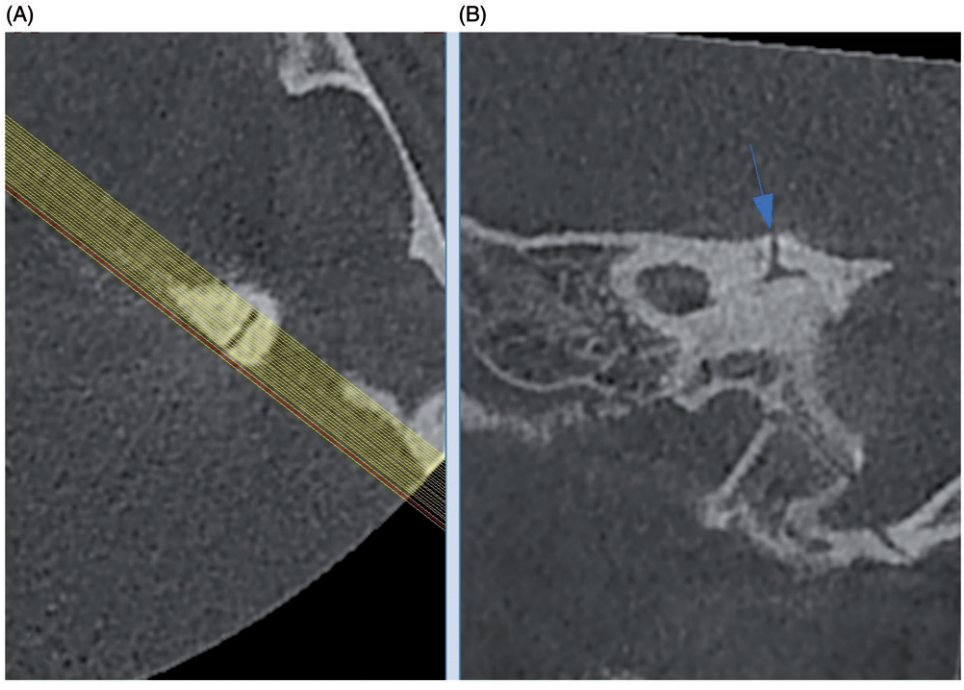

Figure 2. Cone beam computed tomography images. (A) Stenvers plane. Angle of reformation showed on axial CBCT image. (B) Normal features are seen on axial reformatted image.

Intra-observer consistency

A radiologist (S.B.D.) with 5 years of experience performed all measurements. To calculate the intra-observer error rate, randomly selected images were re-evaluated after 1 month and the intraclass evaluation coefficient calculated (0.88).

Statistical analysis

SPSS ver. 20.0 for Windows (SPSS Inc., Chicago, IL) was used for all statistical analyses. The chi-squared test was used to explore differences among the SSCD patterns of the CL/P and control groups; $p \leq .05$ was taken to reflect statistical significance.

Results

We evaluated a total of 129 patients, 53 CL/P patients and 76 controls. The mean age of the CL/P group was 18.42 ± 6.19 years (range 10–34 years) and that of the control group 18.42 ± 6.96 years (range 10–36 years). The mean ages by sex

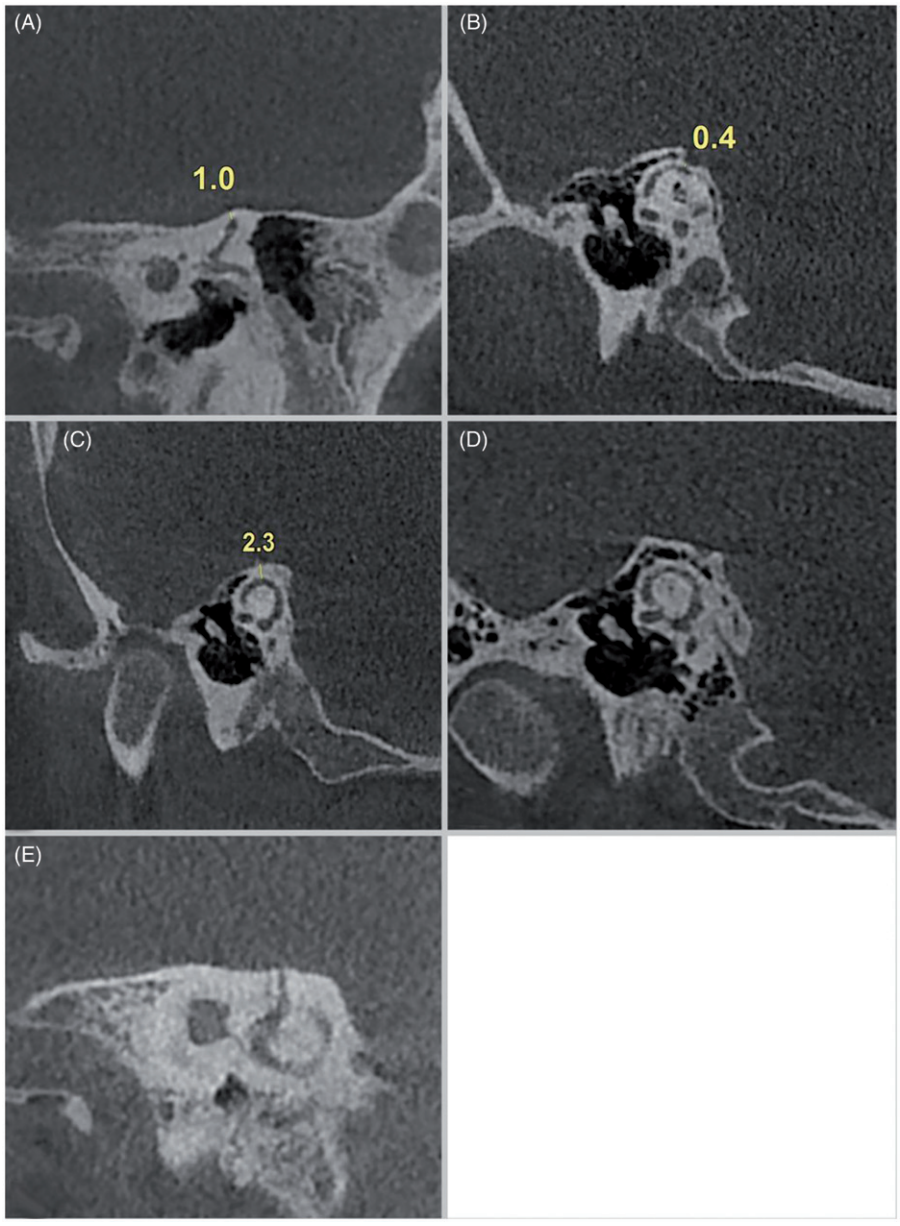

Figure 3. Cone beam computed tomography images show different radiologic features of the superior semicircular canal. (A) Normal. (B) Papyraceous. (C) Thick. (D) Pneumatized. (E) Dehiscent.

Table 1. Mean age of the groups according to gender.

Group	Gender	*N*	Minimum	Maximum	Mean (*SD*)
Cleft group	Male	28	10	34	19.18 (6.77)
	Female	25	10	30	17.56 (5.47)
Control group	Male	42	10	34	21.36 (7.27)
	Female	34	10	36	19.35 (6.49)

are shown in Table 1. A radiologist with 5 years of experience evaluated all 258 temporal bone images from 157 patients following the procedure of Cisneros et al. [17]. In the CL/P group, 53 (50%) cases were described as normal (0.6–1.7 mm in thickness), 20 (19%) as papyraceous (<0.5 mm), 4 (4%) as thick, and 10 (9%) as pneumatized. SSCD was observed in 19 (18%) cases. In the control group, 105 (69%) cases were described as normal (0.6–1.7 mm in thickness), 11 (7%) as papyraceous (<0.5 mm), 4 (3%) as thick, and 24 (16%) as pneumatized. SSCD was observed in 8 (5%) cases. In all, 158 (61%) cases were described as normal (0.6–1.7 mm in thickness), 31 (12%) as papyraceous (<0.5 mm), 8 (3%) as thick, and 34 (13%) as pneumatized. SSCD was observed in 27 (11%) cases. Significant between-group differences were evident in terms of SSCC morphology ($p < .001$) (Table 2).

Discussion

CL/P is a common birth abnormality, evident in 1/800–1000 non-syndromic patients. Middle ear and mastoid problems are common in CL/P patients [1,3,35], as is Eustachian tube dysfunction. The Eustachian tube ensures ventilation of the pressure between the middle ear and mastoid space, affords middle ear protection, and clears middle ear secretions. Eustachian tube dysfunction creates negative pressure in the middle ear space. Such dysfunction may progress to otitis media and atrophy or scarring of the tympanic membrane

Table 2. Distributions of the SSCD patterns in the cleft group and control group.

	Normal *N* (%)	Papyraceous *N* (%)	Dehiscent *N* (%)	Thick *N* (%)	Pneumatized *N* (%)	Total *N* (%)	*p*
Cleft group	53 (50)	20 (19)	19 (18)	4 (4)	10 (9)	106 (100)	<.001
Control group	105 (69)	11 (7)	8 (5)	4 (3)	24 (16)	152 (100)	
Total	158 (61)	31 (12)	27 (11)	8 (3)	34 (13)	258 (100)	

Chi-square $p < .001$.

under either positive or negative pressure [36]. CL/P patients frequently exhibit hearing problems, particularly conductive hearing loss attributable to otitis media with effusion [31,37,38]. Several factors affect such hearing problems, including sex, age, ethnicity and cleft pathology type [39]. In the literature, conductive hearing loss was evident in 12.1–83% of CL/P patients. Flynn et al. [31] reported an incidence of 83%, and Handzic-Cuk et al. [32] an incidence of 59.7%. Another study of 50 CL/P patients found that 59.6% had middle ear effusion and 12.1% symptomatic hearing loss [37]. In a study comparing CL/P patients with healthy controls, the prevalence of SSCD was higher in patients with chronic otitis media [36]. Both audiological and otorhinolaryngological examinations are necessary for CL/P patients [1,36,40].

The etiology of SSCD remains controversial. Nadgir et al. [30] considered that SSCD was not congenital. However, other studies claimed that SSCD was indeed congenital [41,42]. Various genetic factors may cause SSCD. In addition, in adults (especially the obese), SSCD may be caused by sudden alterations in middle ear pressure, highly pulsatile midcranial pressure, trauma to the superior petrosal sinuses or the sigmoid or arachnoid granulations, direct injury to the SSCC and other causes. Alternatively, SSCD may be caused by a disturbance in bone deposition during development. Carey et al. [33] considered that the symptoms and signs of SSCD first developed in adulthood and suggested that trauma or increased cerebrospinal fluid pulsation caused by a rise in intracranial pressure can trigger SSCD [33]. Kurt et al. [6] found that patients with temporomandibular joint symptoms had a higher frequency of SSCD than normal patients, and emphasized that temporomandibular joint symptoms should also be sought when clinicians detect any SCCD symptom. We found that CL/P patients had a higher rate of SSCD than normal patients.

Chausse, in 1943, was the first to image the SSC; various projections thereof were later described [6]. Recently, high-resolution CT of the temporal bone has become an accepted means to image the SSC. However, several studies found that CT overestimated the rate of dehiscence. The middle ear anatomy is complex and is difficult to analyze via CT alone. CT is helpful when exploring the middle ear space and labyrinth. Although CT slices may be very thin, CT is not an excellent imaging technique. Sequeira et al. [15] showed that, especially when SSCD is associated with low-level dehiscence, routine CT cannot be accepted as the gold standard. Tavassolie et al. [21] emphasized that multislice CT can overestimate the extent of SSCD, and thus should not be used to diagnose the condition. Cloutier et al. [39] considered that CT overdiagnosed SSCD. Masaki [43] used helical CT to evaluate 164 ears and concluded that 80% of the SSCD cases diagnosed via CT alone might be false-positives.

Few studies of CBCT imaging of the SSC have appeared. Kurt et al. [6] and Dalchow et al. [27] used CBCT to diagnose SSCD, as did we, because of the low radiation dose, small voxel size, and high spatial resolution. CBCT is very useful to image small anatomical structures. In an *in vitro* study, Bremke et al. [29] emphasized that CBCT was significantly better than high-resolution CT in terms of identifying thin bony coverage of the SSC in temporal bone specimens. Thus, we confirmed earlier reports to the effect that CBCT is better than CT when evaluating bony structures of the middle ear.

Conclusions

CL/P patients have significant otological problems, and SSCD is more common in such patients than the normal population. Thus, SSCD should be considered if a CL/P patient exhibits a vestibular system deficiency. CBCT is associated with a lower radiation dose, better spatial resolution, and thinner slices than CT. Oral and maxillofacial radiologists should pay attention to otological structures when interpreting CBCT images. Future studies should focus on the cleft site and SSCC morphology in larger populations using CBCT, which affords high-level spatial resolution.

Acknowledgement

There is no funding to report for this manuscript.

Disclosure statement

No potential conflict of interest was reported by the authors.

References

[1] Calzolari E, Pierini A, Astolfi G, et al. Associated anomalies in multi-malformed infants with cleft lip and palate: an epidemiologic study of nearly 6 million births in 23 EUROCAT registries. Am J Med Genet A. 2007;143A:528–537.

[2] Sadler TW. Langman's medical embryology. Pheledelphia: Lippincott Williams & Wilkins; 2011.

[3] Sekhon PS, Ethunandan M, Markus AF, et al. Congenital anomalies associated with cleft lip and palate – an analysis of 1623 consecutive patients. Cleft Palate Craniofac J. 2011;48:371–378.

[4] Starbuck JM, Ghoneima A, Kula K. Bilateral cleft lip and palate: a morphometric analysis of facial skeletal form using cone beam computed tomography. Clin Anat. 2015;28:584–592.

[5] Starbuck JM, Ghoneima A, Kula K. A multivariate analysis of unilateral cleft lip and palate facial skeletal morphology. J Craniofac Surg. 2015;26:1673–1678.

[6] Kurt H, Orhan K, Aksoy S, et al. Evaluation of the superior semicircular canal morphology using cone beam computed

tomography: a possible correlation for temporomandibular joint symptoms. Oral Surg Oral Med Oral Pathol Oral Radiol. 2014;117:e280–e288.
[7] Dieterich M, Brandt T. Vestibular system: anatomy and functional magnetic resonance imaging. Neuroimaging Clin N Am. 2001;11:263–273.
[8] Curtin HD. Superior semicircular canal dehiscence syndrome and multi-detector row CT. Radiology. 2003;226:312–314.
[9] Meiklejohn DA, Corrales CE, Boldt BM, et al. Pediatric semicircular canal dehiscence: radiographic and histologic prevalence, with clinical correlation. Otol Neurotol. 2015;36:1383–1389.
[10] Ceylan N, Bayraktaroglu S, Alper H, et al. CT imaging of superior semicircular canal dehiscence: added value of reformatted images. Acta Otolaryngol. 2010;130:996–1001.
[11] Minor LB, Solomon D, Zinreich JS, et al. Sound- and/or pressure-induced vertigo due to bone dehiscence of the superior semicircular canal. Arch Otolaryngol Head Neck Surg. 1998;124:249–258.
[12] Minor LB, Carey JP, Cremer PD, et al. Dehiscence of bone overlying the superior canal as a cause of apparent conductive hearing loss. Otol Neurotol. 2003;24:270–278.
[13] Crovetto de la Torre MA, Whyte OJ, Cisneros Gimeno AI, et al. Superior semicircular canal dehiscence syndrome. Embryological and surgical consideration. Acta Otorrinolaringol Esp. 2005; 56:6–11.
[14] Mondina M, Bonnard D, Barreau X, et al. Anatomo-radiological study of the superior semicircular canal dehiscence of 37 cadaver temporal bones. Surg Radiol Anat. 2013;35:55–59.
[15] Sequeira SM, Whiting BR, Shimony JS, et al. Accuracy of computed tomography detection of superior canal dehiscence. Otol Neurotol. 2011;32:1500–1505.
[16] Manara R, Lionello M, de Filippis C, et al. Superior semicircular canal dehiscence: a possible pathway for intracranial spread of infection. Am J Otolaryngol. 2012;33:263–265.
[17] Cisneros AI, Whyte J, Martinez C, et al. Radiological patterns of the posterior semicircular canal. Surg Radiol Anat. 2014;36:137–140.
[18] Belden CJ, Weg N, Minor LB, et al. CT evaluation of bone dehiscence of the superior semicircular canal as a cause of sound- and/or pressure-induced vertigo. Radiology. 2003;226:337–343.
[19] Krombach GA, Di Martino E, Martiny S, et al. Dehiscence of the superior and/or posterior semicircular canal: delineation on T2-weighted axial three-dimensional turbo spin-echo images, maximum intensity projections and volume-rendered images. Eur Arch Otorhinolaryngol. 2006;263:111–117.
[20] Hagiwara M, Shaikh JA, Fang Y, et al. Prevalence of radiographic semicircular canal dehiscence in very young children: an evaluation using high-resolution computed tomography of the temporal bones. Pediatr Radiol. 2012;42:1456–1464.
[21] Tavassolie TS, Penninger RT, Zuniga MG, et al. Multislice computed tomography in the diagnosis of superior canal dehiscence: how much error, and how to minimize it? Otol Neurotol. 2012;33:215–222.
[22] Stimmer H, Hamann KF, Zeiter S, et al. Semicircular canal dehiscence in HR multislice computed tomography: distribution, frequency, and clinical relevance. Eur Arch Otorhinolaryngol. 2012;269:475–480.
[23] Demirel O, Kaya E, Üçok CÖ. Evaluation of mastoid pneumatization using cone-beam computed tomography. Oral Radiol. 2014;30:92–97.
[24] Hanzelka T, Dusek J, Ocasek F, et al. Movement of the patient and the cone beam computed tomography scanner: objectives and possible solutions. Oral Surg Oral Med Oral Pathol Oral Radiol. 2013;116:769–773.
[25] Teymoortash A, Hamzei S, Murthum T, et al. Temporal bone imaging using digital volume tomography and computed tomography: a comparative cadaveric radiological study. Surg Radiol Anat. 2011;33:123–128.
[26] Fakhran S, Alhilali L, Sreedher G, et al. Comparison of simulated cone beam computed tomography to conventional helical computed tomography for imaging of rhinosinusitis. Laryngoscope. 2014;124:2002–2006.
[27] Dalchow CV, Knecht R, Grzyska U, et al. Radiographic examination of patients with dehiscence of semicircular canals with digital volume tomography. Eur Arch Otorhinolaryngol. 2013;270:511–519.
[28] Hodez C, Griffaton-Taillandier C, Bensimon I. Cone-beam imaging: applications in ENT. Eur Ann Otorhinolaryngol Head Neck Dis. 2011;128:65–78.
[29] Bremke M, Luers JC, Anagiotos A, et al. Comparison of digital volume tomography and high-resolution computed tomography in detecting superior semicircular canal dehiscence – a temporal bone study. Acta Otolaryngol. 2015;135:901–906.
[30] Nadgir RN, Ozonoff A, Devaiah AK, et al. Superior semicircular canal dehiscence: congenital or acquired condition? Am J Neuroradiol. 2011;32:947–949.
[31] Flynn T, Moller C, Jonsson R, et al. The high prevalence of otitis media with effusion in children with cleft lip and palate as compared to children without clefts. Int J Pediatr Otorhinolaryngol. 2009;73:1441–1446.
[32] Handzic-Cuk J, Cuk V, Risavi R, et al. Hearing levels and age in cleft palate patients. Int J Pediatr Otorhinolaryngol. 1996;37:227–242.
[33] Carey JP, Minor LB, Nager GT. Dehiscence or thinning of bone overlying the superior semicircular canal in a temporal bone survey. Arch Otolaryngol Head Neck Surg. 2000;126:137–147.
[34] Curtin HD, Gupta R, Bergeron TR. Embryology, anatomy, and imaging of temporal bone. In: Som PM, Curtin HD, editors. Head and neck imaging. 5th ed. St Louis (MO): Mosby; 2011. p. 1072.
[35] Dedeoglu N, Altun O, Kucuk EB, et al. Evaluation of the anatomical variation in the nasal cavity and paranasal sinuses of patients with cleft lip and palate using cone beam computed tomography. Bratisl Lek Listy. 2016;117:691–696.
[36] Cho YW, Shim BS, Kim JW, et al. Prevalence of radiologic superior canal dehiscence in normal ears and ears with chronic otitis media. Laryngoscope. 2014;124:746–750.
[37] Paradise JL, Bluestone CD, Felder H. The universality of otitis media in 50 infants with cleft palate. Pediatrics. 1969;44:35–42.
[38] Cheong JP, Soo SS, Manuel AM. Factors contributing to hearing impairment in patients with cleft lip/palate in Malaysia: a prospective study of 346 ears. Int J Pediatr Otorhinolaryngol. 2016;88:94–97.
[39] Cloutier JF, Belair M, Saliba I. Superior semicircular canal dehiscence: positive predictive value of high-resolution CT scanning. Eur Arch Otorhinolaryngol. 2008;265:1455–1460.
[40] Berryhill W. Otologic concerns for cleft lip and palate patient. Oral Maxillofac Surg Clin North Am. 2016;28:177–179.
[41] Zhou G, Ohlms L, Liberman J, et al. Superior semicircular canal dehiscence in a young child: implication of developmental defect. Int J Pediatr Otorhinolaryngol. 2007;71:1925–1928.
[42] Chen EY, Paladin A, Phillips G, et al. Semicircular canal dehiscence in the pediatric population. Int J Pediatr Otorhinolaryngol. 2009;73:321–327.
[43] Masaki Y. The prevalence of superior canal dehiscence syndrome as assessed by temporal bone computed tomography imaging. Int J Pediatr Otorhinolaryngol. 2011;131:258–262.